Available online at www.sciencedirect.com

ScienceDirect

Procedia Manufacturing 34 (2019) 535–544

Procedia MANUFACTURING

www.elsevier.com/locate/procedia

47th SME North American Manufacturing Research Conference, Penn State Behrend Erie, Pennsylvania, 2019

A Reverse CAD Approach for Estimating Geometric and Mechanical Behavior of FDM Printed Parts

Baltej Singh Rupal[a*], Khaled G. Mostafa[a*], Yeping Wang[b*], Ahmed Jawad Qureshi[a†]

[a]*Additive Design and Manufacturing Systems Laboratory (ADaMS Lab), Department of Mechanical Engineering, University of Alberta, Edmonton, Canada*
[b]*Laboratory for Computational Sensing and Robotics, Johns Hopkins University, Baltimore, USA*

[*]These authors made equal Contributions [†]Corresponding author. Tel.: +1-780-492-3609; E-mail address: ajquresh@ualberta.ca

Abstract

Fused Deposition Modeling (FDM) printed parts are widely used in various applications. To avoid material and time wastage, it is necessary to assess the geometric and mechanical behavior of the part beforehand. The geometric and mechanical behavior of FDM printed parts is analyzed by various virtual and experimental approaches. The virtual approaches are based on analytical models, which take solid computer-aided design (CAD) models or STL files as input for the analysis. However, in reality, the input CAD model is converted to a combination of slices (toolpath) before it is sent to print. The difference between the CAD and the toolpath model creates a research gap for estimating the properties accurately. The reason being that the printed part is not the replica of the original CAD model but of the sliced model which is dependent on various slicing parameters. This paper presents a novel algorithm, which is capable of converting the sliced file back to a CAD model (called the Reverse CAD model). The Reverse CAD model is capable of providing an accurate assessment of the geometric and mechanical behavior of the printed part as it also incorporates the effect of slicing parameters. In order to validate the algorithm, primitive geometries are printed, and their geometric deviation and mass properties are compared to the Reverse CAD model. Standardized tensile test specimens are also printed with two different materials to compare the experimental mechanical behavior with the finite element analysis of the Reverse CAD model. Comparative studies validate the Reverse CAD model as a better and more accurate estimator of the FDM printed part properties.

Keywords: Additive Manufacturing; Fused Deposition Modeling; Geometric Quality; Mechanical Properties; Reverse Engineering

1. Introduction

Additive manufacturing (AM) is a layer-by-layer material addition process used for manufacturing a wide range of industrial and other applications. As the AM technology is refining, it is taking over the conventional manufacturing processes [1]. Fused Deposition Modeling is a low-cost and a versatile AM process [3], has the potential to offer alternatives to processes such as plastic molding, injection molding, etc. to produce quality plastic products. For FDM to be used in applications such as user end-products, industrial components, it is of extreme importance to develop methods to estimate and assess the output part properties before printing the part. It will allow design requirement analysis, as well as reduce print failure and material wastage. The output quality characteristics of FDM printing such as geometric or dimensional accuracy and mechanical properties rely mainly on the process and machine parameters [2, 3]. The FDM process and the major parameters involved are described below.

1.1. FDM Process and Parameters

The FDM process involves converting the CAD model into a tessellated file format, which facilitates slicing the model into layers. The slicing is done by a dedicated computer-aided manufacturing (CAM) based software before the file is

10.1016/j.promfg.2019.06.217

converted to a toolpath. Finally, the material (in filament form) is extruded on the print bed according to the prescribed toolpath to fabricate the part. The range of materials and printed part sizes is rather vast, ranging from simple polymers such as Nylon-12, Polycarbonate (PC), and Acrylonitrile Butadiene Styrene (ABS), to highly sophisticated and high-strength materials like carbon fiber or metallic composites, including special purpose materials. The major process parameters include the STL file resolution, slicing parameters, and machine parameters such as the bed temperature, extruder speed, etc.

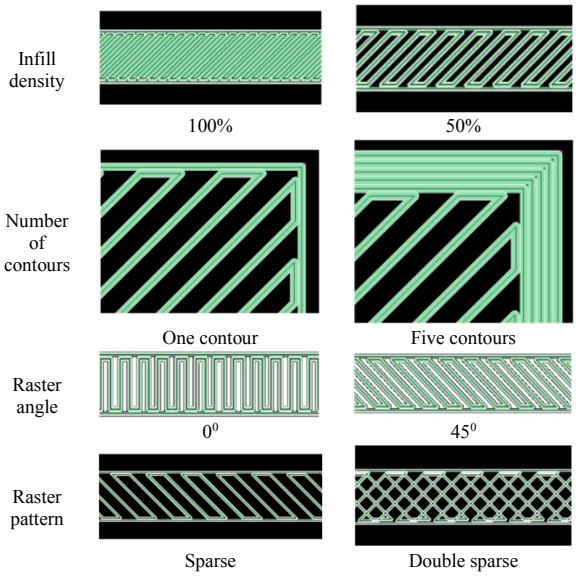

Fig. 1. Depiction of various process parameters used in the study [25]

The important slicing parameters used in this study to realize the Reverse CAD model are shown in Fig. 1 and explained below. As discussed in the introduction, there are different slicing parameters, but due to the limitations of the slicer used in this study only few parameters were manipulated. However the reverse CAD algorithm works with any slicer as it only reads the output G-code.

Description of the slicing process parameters:

- Infill density: The percentage measure of the area of the layer to be printed to the total area of the layer.
- Number of contours: Number of boundaries around each layer to increase the stability and mechanical behavior of the part.
- Raster angle/orientation: Angle between one of the axes and the direction of the raster.
- Raster pattern: There are two types of raster patterns – sparse and double sparse. In sparse patterns, the orientation or the raster angle remains the same for all layers. For double sparse patterns, the raster angle shifts by 90^0 after each layer.
- Number of Shells: Number of upper and lower covers (surfaces) with 100% infill density to make the part solid even if it has less infill density inside. (Not shown)

Due to a number of unknown variables and process parameters, challenges arise in achieving the desired geometric and mechanical properties of the printed components. In order to make the FDM process industrially robust, it is important to investigate the effect of these parameters and the relationship between them [1]. Recent literature studies on the quantification and prediction of geometric and mechanical properties for the FDM process are discussed in the following sections respectively, and their limitations are highlighted.

1.2. Geometric Quality

Geometric quality prediction of the FDM printed part is usually based on experimental studies and analytical models. The experimental studies are usually performed on different types of benchmark test samples [4], and process parameters are varied according to designed or repeated experiments. Shahrain et al. [5] considered 13 process parameters for the FDM process and employed a Taguchi-based experimental design to a test artifact in order to check various geometric quality characteristics such as dimensional deviation, flatness, and cylindricity. The results show that dimensional deviation, component size, and platform temperature were the most critical process parameters. However, for a summation metric of various Geometric Dimensioning and Tolerancing (GD&T) based geometric characteristics, the essential parameters turned out to be extruder temperature and layer thickness. Another study of the FDM process by Mohamed et al. [6] performed optimization of the process parameters for dimensional accuracy using I-optimality criterion. The research claims that layer thickness and air gap are the most significant parameters concerning dimensional accuracy. They also developed a prediction model using quadratic regression, whose results are in good agreement with confirmation experiments. Similarly, more studies [7-10] conducted using various experimental and optimization techniques provide an estimation methodology of the geometric quality of the 3D printed parts.

Certain research studies based on analytical models also claim to have achieved a good estimation for geometric accuracy of FDM parts. Zhu et al. [11] modeled the effect of the CAD to STL conversion on the dimensional accuracy based on contour point displacement. Geometric deviations from random variations are also considered by using a random field theory, and a good prediction of repeatable and random deviations is represented using polar and radial functions. Another research work [12] modeled the volumetric accuracy of the AM printed parts by conducting a parametric evaluation of the geometric errors based on experimental data. The parametric error functions for the process were developed, and the results were validated for 2D models. Similar studies provide experimental-based models [13-15] and analytical models [16] for estimating the geometric accuracy of the AM process.

The primary issue with the experimental testing of the geometric properties is that it is time-consuming, inhibits the 3D printer from printing the actual products, and requires extensive material resources. Furthermore, additional equipment, such as co-ordinate measuring machines (CMM) and laser scanners for testing the geometric behavior, is needed. Analytical and modeling methods on the other hand are more sustainable and do not lead to material wastage and downtime.

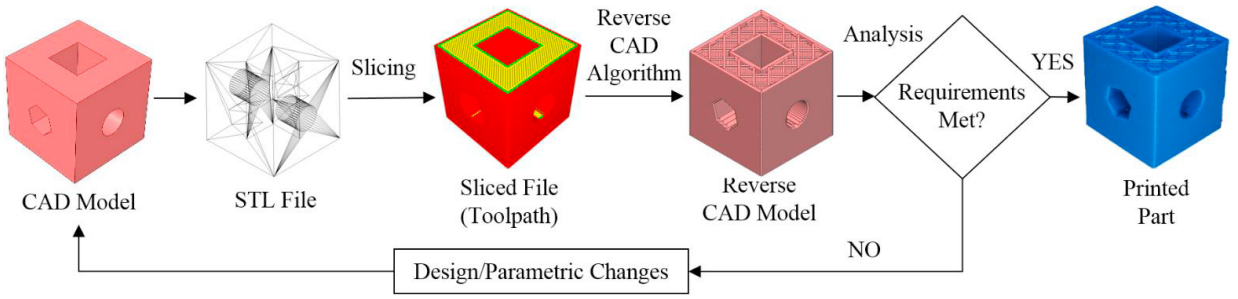

Fig. 2. A flowchart depicting the output property prediction methodology based on the Reverse CAD algorithm

However, current modeling methodologies fail to provide an accurate deviation map of the geometric quality of the FDM printed parts. This is due to the fact that most models ignore the slicing parameters and no methodology has attempted to incorporate these parameters into the virtual analysis. Since slicing parameters also affect the output geometric quality as proven by experimental studies, the modeling methodologies should also incorporate them.

1.3. Mechanical Quality

The FDM process introduces mechanical anisotropic behavior to the manufactured part even when the filament used is of isotropic material. These anisotropic mechanical properties are variable, and each of them is a function of the part orientation, infill percentage, raster orientation, raster pattern, and layer thickness [17-19]. To currently predict the mechanical behavior of FDM manufactured parts, researchers use either Design of Experiments (DOE) approaches to find best-fit regression [20-21] models or finite element analyses (FEA) with 100% solid CAD models [22]. Each technique has its advantages and disadvantages, but neither of them can predict mechanical behavior generically and conveniently without depending on specific geometries or a certain range of parameters.

Using DOE methods enables researchers to determine the most significant process parameters affecting the mechanical behavior of the selected material, parameters levels, and part geometry [23-24]. The most significant process parameters studied in selected articles ranging from 2001 to 2017 are summarized and ranked in [2, 25], and the most important parameters are then analyzed again to create a regression model to predict the mechanical properties and cost. Moreover, different regression models were presented based on significant parameters [17, 20-22, 27] and multi-objective optimization [23-24, 25, 28-29]. The studies above use standardized testing specimens to measure and optimize the mechanical properties; other studies use product-based optimization [29-30]. In product-based optimization, the performance of the product is the primary objective and is tweaked by manipulating the process parameters. In [29] for instance, the aim was to optimize the range of an FDM manufactured catapult, where the throwing distance depended explicitly on the part elasticity and the yield strength. The main disadvantage of this prediction method is that for the same parameters (geometry, process, and material), the scalability of the part affects the prediction [3].

A constitutive model was presented to predict the mechanical behavior based on an orthotropic behavior stiffness matrix, and the constants are evaluated experimentally in [31]. Also, several analytical models to predict the strength of the part in terms of the bonding between filaments, raster, and part orientation were developed and experimentally validated in [32-35]. Various studies used FEA with different modeling philosophies to simulate the stresses along simple tensile test specimens [36-38]. In [36], the orthotropic material stiffness matrix was experimentally evaluated, and the FEA model used was a complete solid part. Rezayat et al. [37] performed an FEA for several single-layered FDM parts, where each layer had a different raster orientation, and then calculated the effective stress for the overall part. A semi-realistic approach was presented in [38], in which a full standard tensile specimen was 3D modeled using 100% infill density layers with two alternating raster orientations per layer, where the 3D air gaps were geometrically included. The main disadvantages of the previously discussed FEA methods include that they require extensive material characterization to represent the orthotropic behavior and that they are limited to simple linear raster patterns and 100% infill density parts. A tool path generation using cladding and milling commercial software was presented in [39] to visualize the part exteriors and interiors for any geometry, but it was applied to visualize the toolpath only.

For both geometric and mechanical quality prediction, the methods discussed above have their strengths and weaknesses. However, none of the methods predict the effect of the STL to slicing file conversion on the properties of the printed part. Since the properties of the printed part are dependent on the slicing parameters as well, it is of great importance to include that parameters in any virtual analysis to predict the output properties. Process parameters related to the slicing of the STL file such as the number of contours, air gaps, hatch spacing, and infill density will be considered for the prediction purposes. For example, it has been proven experimentally that variation in infill has a drastic effect on the mechanical properties [25] and geometric properties [5] of the printed part.

The need for a reference, to compare the FDM manufacturing errors to, derived the authors to develop the

'Reverse CAD algorithm'. This algorithm provides a 'theoretical ideal replica of the printed part' which includes the intrinsic FDM manufacturing errors/stamp such as the layers waviness from the sides, filament pattern curvature from the top and bottom, and part orientation. During the FDM process other uncontrolled manufacturing errors happens due to material viscosity, nozzle and bed temperature effects, warpage, nozzle speed, positioning accuracy, and other uncontrolled errors. By comparing the final manufactured part shape to the original input CAD file is not completely correct as the FDM Stamp/intrinsic errors will always be there. The reverse CAD algorithm can be used to optimize the slicing parameters to minimize the intrinsic errors/stamp, and by comparing the manufactured part to the reversed CAD model the uncontrolled process errors can be optimized.

This research work focuses on quantifying the issues related to the sliced file and its effect on the final print quality using virtual methods without experimentation. This will be realized by developing an algorithm which is capable of converting the sliced file (toolpath) back into a solid CAD model called the Reverse CAD model. The methodology for the work is shown in Fig. 2. The generic AM process chain is modified. A geometric and mechanical analysis is performed on the Reverse CAD model to check the model for design requirements. If the conditions are met, then the sliced file is sent to print. Otherwise, design changes or parametric variations are made to meet the design criteria. The Reverse CAD algorithm is explained in detail in Section two. The geometric and mechanical quality assessment results are discussed in Section three and four respectively. Since this article conducts an initial validation of the algorithm, the geometric quality comparisons are preformed based on visual inspections of the images and for mechanical quality only elastic behavior is compared. Finally, the conclusions and future scope are described in Section five.

2. Methodology

The FDM process starts by slicing the CAD file in order to be additively manufactured with respect to the required process parameters using a pre-processing slicer software. The output of the slicing software is a G-code for the extruder nozzle path. The reverse CAD algorithm, which is demonstrated in Fig. 3, is written in the MATLAB environment. It reads the output G-code and the constants values; for example, the layer thickness and the road width are fed into it. It then calculates the deposited filament cross section parameters using equations (1) to (7). The deposited filament is assumed to ellipse, as shown in Fig.3, based on previous studies which used microscopy imaging to analyze the filament profile and used the ellipse to analytically model mechanical and geometrical behavior [19, 41-43]. The deposited filament has l_a as the major radius and l_b as the minor radius of the ellipse, while w is the road width and r is the overlap ratio between adjacent filaments. lth is the layer thickness value used for FDM printing. Where S_1 is the surface area of the filament before deposition, where D is the extruder nozzle diameter, and f is the shrinkage value after deposition and cooling off. S_2 is the surface area of the ellipse of the deposited filament. By equating S_1 and S_2 and using equation (1) and (2), the ellipse radii and the overlap ratio are computed.

$$l_a = \frac{w \times r}{2} \tag{1}$$

$$l_b = \frac{lth \times r}{2} \tag{2}$$

$$S_1 = \frac{D^2 \times \pi}{4} \times f \tag{3}$$

$$S_2 = l_b \times l_a \times \pi \tag{4}$$

$$r = \sqrt{\frac{D^2 \times f}{w \times lth}} \tag{5}$$

$$l_a = \sqrt{\frac{D^2 \times f \times w}{4 \times lth}} \tag{6}$$

$$l_b = \sqrt{\frac{D^2 \times f \times lth}{4 \times w}} \tag{7}$$

The algorithm scans the code line by line and searches for the different G-codes that correspond to different printing actions. There are two main modes in the FDM process: in the first mode, the extruder moves without printing in a fast approach motion, while in the second mode, it extrudes material with a certain linear speed. If the Reverse CAD model is required without the support materials, the code will discard any path for the support or the interface material. If the second printing mode is detected and the path is either a contour, a raster infill, or a shell, an Application Programming Interface (API) sequence syntax writing function is called in order to export the syntax used by the CAD software to generate a corresponding 3D model for the extruded path. The API collects the starting and end points of the current printing path and writes a syntax to create a plane at the start point and perpendicular to the required path. Then another syntax is created to sketch an ellipse on the previous plane using the previously calculated parameters. After that, a syntax is written for the extrusion boss/base of the created ellipse with an extrusion length correspondent to the difference between the start and end point of the printed line trajectory. The extruded ellipse geometries are combined together as one part only at their intersection areas as shown in Fig. 3, while the resultant voids between the non-intersecting ellipses are kept in the reverse CAD model. The last syntax is written to create a revolve feature between the currently printed line and the previous line, fill in the sharp gap developed, and to simulate the filament bending between two tool paths intersecting at an angle. After a layer ends in the G-code, the algorithm shifts the z coordinates in the vertical direction by the layer thickness value.

The algorithm exports a file containing sequenced API syntaxes after it determines that the printing of the part is finished in the G-code. In the CAD software, the API launcher is used to open the syntax file and the part is 3D modeled as instructed in the initial G-code. Finally, a CAD file is exported and can be opened with any CAD software and used to analyze the properties of the part.

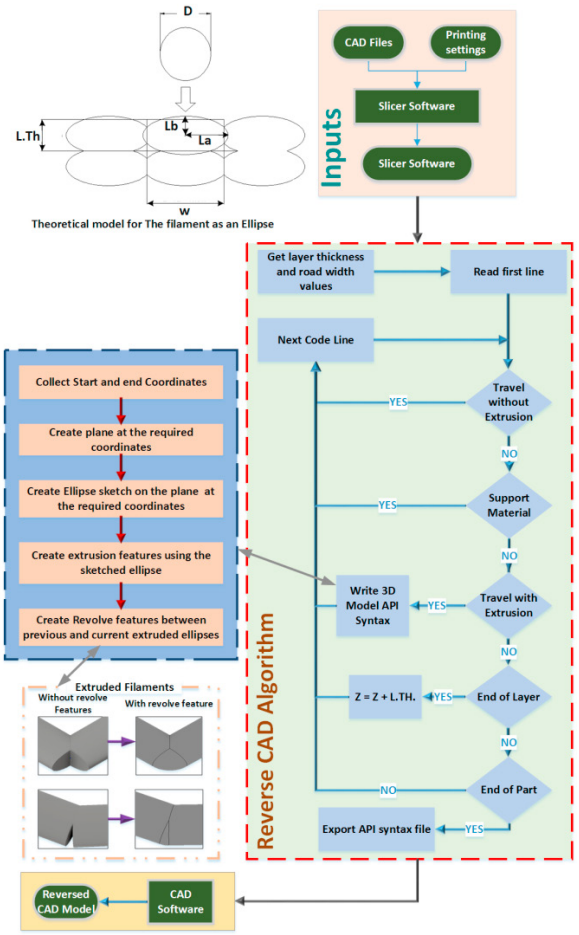

Fig. 3. The Reverse CAD algorithm

The time to convert the exported G-code into an API syntax file is negligible compared to the time to convert the API syntax into a reversed CAD model. The time consumed to create a reversed CAD model consisting of 700 features, like extrusions and revolves, with their sketches is around 1hour. It was noticed and then experimented that as the number of features per part increase the time consumed to create the next feature within the same part takes longer time, for example the creation time of the of the feature with the sequence number of 100 is 1 s while the feature with the sequence number 400 is 3 s and the 700th features takes 8 s. The whole operation was done on a computer of 16 GB memory and Core I7 Processor with 4GHz capacity.

3. Geometric Quality Results

CAD models of primitive geometries with small features were selected to demonstrate the working of the algorithm. Reverse CAD models were generated for the designed models using the algorithm. A cube was modeled, saved as an STL file, and a slicing file was created. A sparse infill pattern was selected for the cubical part as well as a 45^0 raster angle. Similarly, a cylindrical part was modeled and saved as a slicing file. The critical process parameters for both of the parts are depicted in Table 1.

Table 1. Printing Parameters for experimentation

Parameters	Cube	Cylinder
Infill pattern	Sparse	Double sparse
Number of contours	5	4
Raster angle	45^0	0^0
Layer thickness (mm)	0.33	0.33
Number of shells	1	1
Infill density	50%	100%

The slicing files for both the parts were fed into the Reverse CAD algorithm, and the Reverse CAD models were generated. The infills density of the outer shell used is set lower than 100% in order to depict the capability of the algorithm in a better way. Finally, the parts were printed using a Stratasys F370 FDM printer and compared to the Reverse CAD model through visual inspection. The Reverse CAD model, and the corresponding printed parts are shown in Fig. 4. The layers, infill spaces, shells, and contours depicted in the Reverse CAD models are the same as in the printed parts. Now that we have established that the algorithm can generate an accurate virtual model of the part to be printed, we are moving forward with the analysis.

First, the mass properties of the Reverse CAD models and the final printed parts were compared to obtain confidence in the applicability of the Reverse CAD models for virtual analysis.

Table 2. Mass comparison Table

Mass comparison (grams)	Cube	Cylinder
Original CAD Model (A)	11.97	9.17
Reverse CAD model (B)	7.711	8.618
Printed Part (C) (Average)	6.758	7.738
Percentage difference (|C-A|*100/C)	77.12	18.50
Percentage difference (|C-B|*100/C)	14.10	11.37

To check the effect of the slicing parameters on the mass properties of the printed parts, a mass comparison study was conducted. It involved assigning the same material (ABS plastic in this case) to the Reverse CAD model and calculating the mass properties of the model virtually. A comparison between the mass of the initial CAD model (A), Reverse CAD model (B) and the printed part (C) average was conducted, and the results are shown in Table 2. A percentage difference between the mass properties was calculated.. The cube's infill pattern was sparse and the cylinder's infill pattern was double sparse. Still, the Reverse CAD predicted the mass properties accurately, regardless of the infill settings. For example, it is clear from the 77% difference that the initial CAD model cannot provide a satisfactory estimation of the mass properties of the printed part, which has a 50% infill density. The difference reduces to only 14.1% when compared with the Reverse CAD model. It is worth mentioning that the mass variability between the same printed parts are within +/- 0.2 grams This type of study can prove critical when the mass of the part is one of the important design criteria. The difference between the properties of the material assigned in the software and actual material is the reason for the 10-15% difference between the Reverse CAD model and the actual part mass properties.

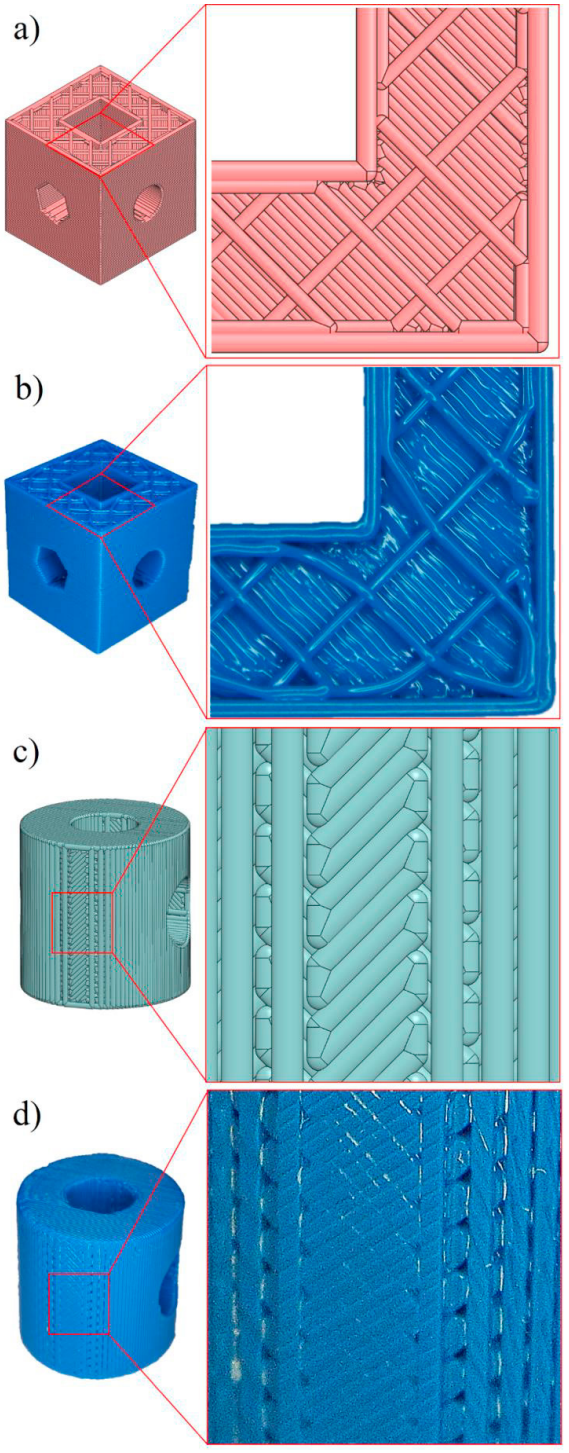

Fig. 4. a) Cubic Reverse CAD model: isometric and zoomed-in view
b) The printed cubic part: isometric and zoomed-in view
c) Cylindrical Reverse CAD model: isometric and zoomed-in view
d) The printed cylindrical part: isometric and zoomed-in view

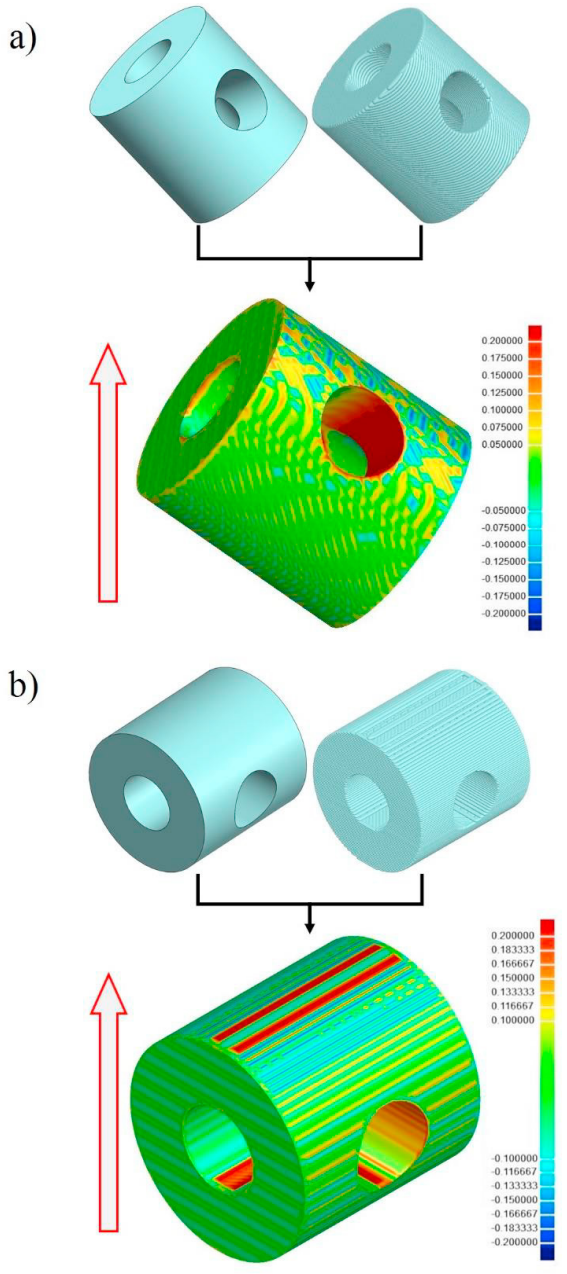

Fig. 5. Geometric deviation analysis for the CAD model vs. Reversed CAD model of the cylindrical part
a) Build orientation 1: cylinder axis aligned to print bed
b) Build orientation 2: cylinder axis parallel to print bed

It was observed that as the volume of the CAD model increases, the percentage difference between the Reverse CAD model and printed part decreases, which would make the algorithm more accurate with large volume parts.

A geometric deviation analysis was performed on the Reverse CAD files, and comparisons were conducted with the initial CAD file to check for possible geometric deviations

before printing the part. This not only helped to identify the regions with more geometric deviations, but it also allowed the designer to reorient the part and take into account the slicing parameters to reduce the geocentric deviations. The geometric deviation analysis was performed by using SolidWorks 2018 academic version.

First, the CAD model was opened in SolidWorks. Then the Reverse CAD file was imported into the same workspace using 'Geomagics for SolidWorks'. After that, both models were aligned perfectly with each other and the 'deviation analysis' tool was used to calculate the results. Two cases of different part orientations were considered on the cylindrical part to conduct the analysis. In the first build orientation, the major axis of the cylinder was oriented at 45^0 with respect to the base build plane (see Fig. 5a). For the second build orientation, the axis of the cylinder was rotated 90^0 with respect to the build plane (see Fig. 5b). The corresponding geometric deviations for both the orientations are also shown. Geometric deviations from the range of -0.200 mm to +0.200 mm can be seen in both cases on different locations depending on the orientation. In case 1, the major deviation region is the smaller cylindrical hole perpendicular to the major axis, since the staircase effect is more prominent in that region. In case 2, the staircase effect is seen on top of the part and the lower side of the cylindrical holes. Further detailed and controlled geometric deviation analysis with parametric variations can prove useful for minimizing geometric deviations and parametric optimization for improving the geometric quality.

4. Mechanical Behavior Results

One of the direct applications of the reverse CAD algorithm is to predict the mechanical behavior of FDM additively manufactured parts while considering the process parameters using FEA. Two different configurations were selected as shown in Table 3, based on the previous experimental investigation in [25], to manufacture tensile test specimens (dog bones) with two different materials. The test specimen selected follows ISO 527-2:2012(E) [43], type 1B. The G-codes for these two configurations were also used as an input for the reverse CAD algorithm to generate the Reverse CAD file that has the exact same slicing parameters of the specimen manufactured by the FDM process.

Table 3. FDM process parameters for configuration (i) and (ii)

Configuration	(i)	(ii)
Layer thickness (mm)	0.25	0.33
Filling density (%)	28	10
Number of Contours	3	5
Road width (mm)	0.71	0.71
Raster angle (degrees)	0	45
Number of shells	2	4
Raster Pattern	Double Sparse	

The two materials selected were Nylon-12 and PC. The mechanical behavior of the materials used is assumed isotropic, and the extruded ellipse geometries are combined together as one part only at the intersection areas as shown in Fig. 3, while the resultant voids between the non-intersecting ellipses are kept in the reverse CAD model. The influence of the inter-layer adhesion will not affect the geometric characteristics of the part as a theoretical ideal reference, but it will certainly affect the accuracy of the prediction of the mechanical characteristics in the printing direction. The isotropic properties used in this study are presented in Table 4 and are based on [42].

Table 4. Material properties used in the FEA

Material Property	Nylon-12	PC
Elastic Modulus (MPa)	1000	2050
Poisson's Ratio	0.38	0.32
Density (gm/cm^3)	1	1.3

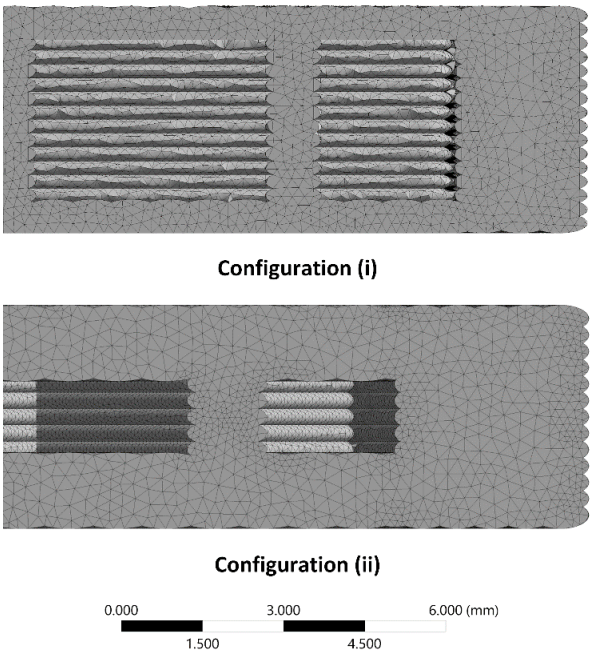

Fig. 6. Half cross section of the shoulder area showing the meshing of configuration (i) and (ii)

Based on these material properties and the process parameters, an experimental study was conducted which will be used for validation purposes. Five tensile test specimen replicates were manufactured per each configuration and material using a Stratasys Fortus 900mc FDM printer. With a 1 mm/min strain rate, the tensile test was performed on an MTS 810 tensile testing machine according to ISO 527-1 [43]. The uncertainty in results ranges between 0.46% and 3.2 %, with a mean of 0.96% and the standard deviation of 0.93%. The average force-displacement curve for each specimen is shown in Fig. 7 (a). The experimental results are compared to the FEA results for the range of 1 mm, which cover the linear elastic zone of the part, and the comparison is depicted in Fig. 7 (b).

For the FEA analysis, the two parts representing the two configurations were meshed using quadratic tetrahedrons with minimum and maximum element sizes of 0.1 and 0.5 mm respectively. The quadratic tetrahedrons capture the bending deformation in the elements on the contrary to the linear ones,

and also show competitive results compared to the hexahedrons elements [45]. It is also easier and faster to mesh complex shapes with tetrahedrons in general. The resultant mesh is shown in Fig. 6, with a total of around 9.5 million elements for both configurations. The overall quality of the generated mesh was assessed by different parameters, with an average mesh quality of 0.9 (where 1 is the maximum quality), the average aspect ratio of 2, and the average element skewness of 0.05 (where 0 is the best skewness).

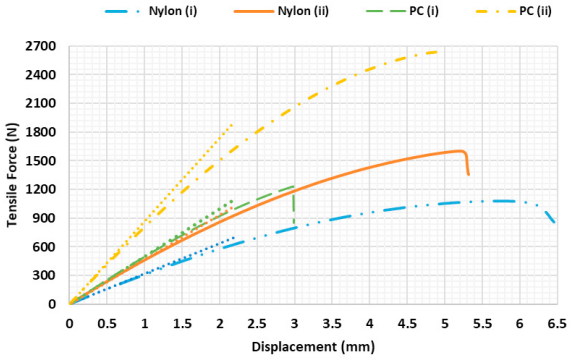

(a)

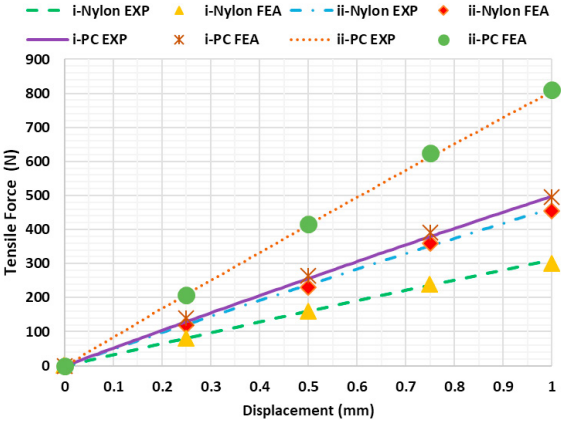

(b)

Fig. 7. (a) Mechanical test results of both Nylon-12 and PC with printing configuration i and ii

(b) Results up to 1 mm displacement compared to the FEA prediction

The boundary conditions used in the FEA are fundamental, where one end of the test specimen was fixed in the x-axis direction and allowed to translate symmetrically around the centerlines of the cross section in the Y and Z axes directions. Then, a four step displacement from 0 to 1 mm with 0.25 increments, was applied to the opposite end to tension the specimen in the positive x-axis direction. The 1 mm range was chosen based on our goal to simulate only the linear elastic zone of the FDM parts. Since the yield strength of plastics is difficult to determine from curves, the simulation zone was determined by plotting the tangent modulus line (dotted lines) between the points corresponding to 0.05% and 0.25% strain as shown in Fig. 7 (a) according to ISO 527-1 [44]. It was observed that the material behaves linearly until about 1mm of the full tested displacement.

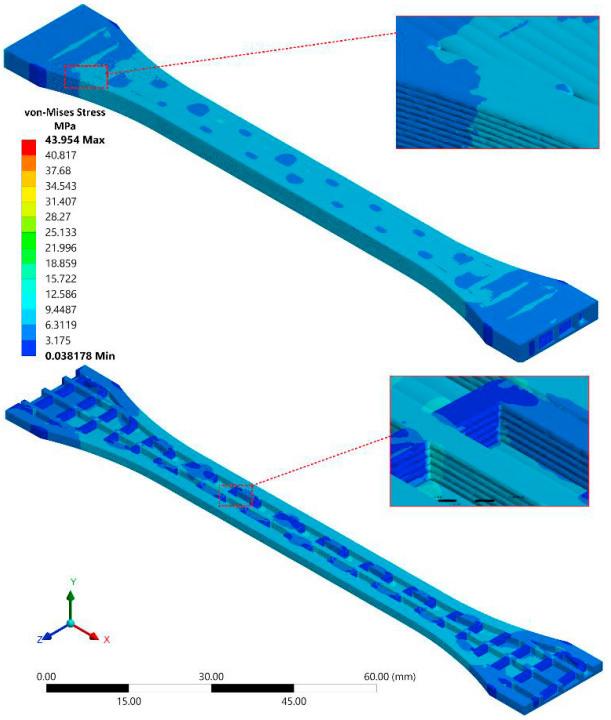

Configuration (i)

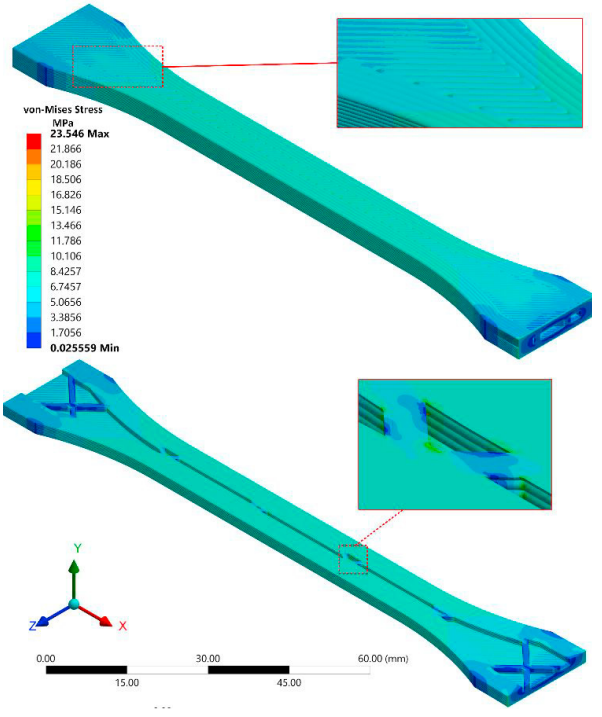

Configuration (ii)

Fig. 8. von Mises stress FEA results for Configuration (i) and (ii) made of Nylon-12. Corresponding section views are shown to depict infills

ANSYS Workbench Academic was used in this study to conduct the FEA. The von Mises stress results of the Nylon specimen manufactured with the configuration (i) and (ii) are shown in Fig. 8, where the stresses are presented on the top surface and throughout a longitudinal section. To validate the results, the reaction force at the fixed end was evaluated for each displacement step, as this can be easily compared to the raw mechanical tensile test results. The FEA analysis was also used to evaluate the stresses and the reaction tensile force for the same two configurations of PC material, while only the Nylon-12 results are shown in Fig. 8. The experimental and FEA force data is shown in Table 5 with a percentage error comparison. The FEA results using reverse CAD model are in good agreement with the experimental results with a maximum of 5.74% error. The FEA of the original CAD is also performed to show the deviation compared to the experimental results. Based on these results, the Reverse CAD approach proves to accurately analyze the imposed anisotropic mechanical behavior of the FDM printed parts of any isotropic material within the linear elastic range and in the perpendicular direction to the printing. The limitation to the current version of the reverse CAD model is that it cannot predict the mechanical properties in the printing direction as the extruded ellipse geometries are combined together as one part only at their intersection zones.

Table 5. Experimental and FEA force data comparison

Displacement (mm)	FEA Force on original CAD (N)	Experimental Force (N)	FEA Force on Reverse CAD (N)	% Error
	Nylon (i)			
0.25	135	84	79.85	4.94
0.5	256	161	159.7	0.81
0.75	370	237.3	237.56	0.11
1	492	309	307.53	0.48
	Nylon (ii)			
0.25	135	119.43	121.36	1.62
0.5	256	228.86	238.53	4.22
0.75	370	357.69	358.29	0.17
1	492	463.6	460.2	0.73
	PC (i)			
0.25	216	122	129	5.74
0.5	460	257	261.2	1.63
0.75	630	381	383.4	0.63
1	830	507	506.4	0.12
	PC (ii)			
0.25	216	211.5	207.14	2.06
0.5	460	416.3	416.34	0.01
0.75	630	612	624.5	2.04
1	830	802	800.21	0.22

5. Conclusions and Future Scope

In the era of AM, novel simulation methods are needed to further reduce the design and production time and to enable engineering the part with required properties through CAD/CAM tools. This paper proposes an innovative tool for simulating the geometric and mechanical properties while using the current generation of open source/commercially available CAD/CAM software.

This is based on a Reverse CAD algorithm, which reconstructs a CAD model from the sliced file. The Reverse CAD model is the virtual replica of the part to be printed with specific printer and machine parameters, e.g., layer thickness, infill density, and so on. The algorithm facilitates accurate modeling and analysis of the FDM printed part behavior. The application and efficiency of the algorithm are validated by geometric comparison, mass comparison, deviation analysis, and mechanical behavior analysis using different process parameters and printers.

The limitation of the algorithm as of now is the computation speed, as the number of features increase in the CAD model, the computational speed decreases. However, the computational speed increases simultaneously to layer thickness, since it takes fewer loops to cover the same volume. Currently, the Reverse CAD algorithm is further developed to reduce computation speed, make it more robust, and also to simulate the support structures to understand the effect of supports on the output properties and to optimize it. The future analysis work will be implementing the plasticity and fracture models in FEA while using the reverse CAD model, and using specimen parts inspired by applications.

Acknowledgments

The authors acknowledge the financial support provided by the Natural Sciences and Engineering Research Council of Canada (NSERC) under grant no. RGPIN-2016-04689. The authors are also thankful to the China Scholarship Council (CSC) for supporting Yeping Wang to be a part of this research project.

References

[1] Gibson I. The changing face of additive manufacturing. J Manuf Technol Manag 2017;28:10–7. doi:10.1108/JMTM-12-2016-0182.

[2] Mohamed OA, Masood SH, Bhowmik JL. Optimization of fused deposition modeling process parameters: a review of current research and future prospects. Adv Manuf 2015;3:42–53. doi:10.1007/s40436-014-0097-7.

[3] Qureshi A., Mahmood S, Wong WL., Talamona D. Design for Scalability and Strength Optimisation for components created through FDM process. Iced 2015 2015:1–12

[4] Rebaioli L, Fassi I. A review on benchmark artifacts for evaluating the geometrical performance of additive manufacturing processes. The International Journal of Advanced Manufacturing Technology. 2017 Nov 1;93(5-8):2571-98.

[5] Shahrain M, Didier T, Lim GK, Qureshi AJ. Fast Deviation Simulation for “Fused Deposition Modeling” Process. Procedia CIRP 2016;43:327–32. doi:10.1016/j.procir.2016.02.004.

[6] Mohamed OA, Masood SH, Bhowmik JL. Optimization of fused deposition modeling process parameters for dimensional accuracy using I-optimality criterion. Measurement. 2016 Mar 1;81:174-96.

[7] Sood AK, Ohdar RK, Mahapatra SS. Improving dimensional accuracy of fused deposition modelling processed part using grey Taguchi method. Materials & Design. 2009 Dec 1;30(10):4243-52.
[8] Nancharaiah T, Raju DR, Raju VR. An experimental investigation on surface quality and dimensional accuracy of FDM components. International Journal on Emerging Technologies. 2010 Jan;1(2):106-11.
[9] Mahmood, S., Qureshi, A.J. and Talamona, D., 2018. Taguchi based process optimization for dimension and tolerance control for fused deposition modelling. Additive Manufacturing, 21, pp.183-190.
[10] Raghunath N, Pandey PM. Improving accuracy through shrinkage modelling by using Taguchi method in selective laser sintering. International journal of machine tools and manufacture. 2007 May 1;47(6):985-95.
[11] Zhu Z, Anwer N, Mathieu L. Deviation modeling and shape transformation in design for additive manufacturing. Procedia CIRP. 2017 Jan 1;60:211-6.
[12] Tong K, Amine Lehtihet E, Joshi S. Parametric error modeling and software error compensation for rapid prototyping. Rapid Prototyping Journal. 2003 Dec 1;9(5):301-13.
[13] Afazov S, Okioga A, Holloway A, Denmark W, Triantaphyllou A, Smith SA, Bradley-Smith L. A methodology for precision additive manufacturing through compensation. Precision Engineering. 2017 Oct 1;50:269-74.
[14] Lieneke T, Denzer V, Adam GA, Zimmer D. Dimensional tolerances for additive manufacturing: Experimental investigation for Fused Deposition Modeling. Procedia CIRP. 2016 Jan 1;43:286-91.
[15] Rupal BS, Ahmad R, Qureshi AJ. Feature-Based Methodology for Design of Geometric Benchmark Test Artifacts for Additive Manufacturing Processes. Procedia CIRP. 2018 Jan 1;70(1):84-9.
[16] Moroni G, Syam WP, Petro S. Towards early estimation of part accuracy in additive manufacturing. Procedia CIRP. 2014 Jan 1;21:300-5.
[17] Chacón, J.M., Caminero, M.A., García-Plaza, E. and Núñez, P.J., 2017. Additive manufacturing of PLA structures using fused deposition modelling: Effect of process parameters on mechanical properties and their optimal selection. Materials & Design, 124, pp.143-157.
[18] Ziemian, C., Sharma, M. and Ziemian, S., 2012. Anisotropic mechanical properties of ABS parts fabricated by fused deposition modelling. In Mechanical engineering. InTech.
[19] Ahn, S.H., Montero, M., Odell, D., Roundy, S. and Wright, P.K., 2002. Anisotropic material properties of fused deposition modeling ABS. Rapid prototyping journal, 8(4), pp.248-257.
[20] Montero, M., Roundy, S., Odell, D., Ahn, S.H. and Wright, P.K., 2001. Material characterization of fused deposition modeling (FDM) ABS by designed experiments. Society of Manufacturing Engineers, 10(13552540210441166).
[21] Chockalingam, K., Jawahar, N. and Praveen, J., 2016. Enhancement of anisotropic strength of fused deposited ABS parts by genetic algorithm. Materials and Manufacturing Processes, 31(15), pp.2001-2010.
[22] Domingo-Espin, M., Puigoriol-Forcada, J.M., Garcia-Granada, A.A., Lluma, J., Borros, S. and Reyes, G., 2015. Mechanical property characterization and simulation of fused deposition modeling Polycarbonate parts. Materials & Design, 83, pp.670-677.
[23] Srivastava, M. and Rathee, S., 2018. Optimisation of FDM process parameters by Taguchi method for imparting customised properties to components. Virtual and Physical Prototyping, pp.1-8.
[24] Srivastava, M., Maheshwari, S., Kundra, T.K. and Rathee, S., 2017. Multi-response optimization of fused deposition modelling process parameters of ABS using response surface methodology (RSM)-based desirability analysis. Materials Today: Proceedings, 4(2), pp.1972-1977.
[25] Mostafa, K.G., Montemagno, C. and Qureshi, A.J., 2018. Strength to cost ratio analysis of FDM Nylon 12 3D Printed Parts. Procedia Manufacturing, 26, pp.753-762.
[26] Padhi, S.K., Sahu, R.K., Mahapatra, S.S., Das, H.C., Sood, A.K., Patro, B. and Mondal, A.K., 2017. Optimization of fused deposition modeling process parameters using a fuzzy inference system coupled with Taguchi philosophy. Advances in Manufacturing, 5(3), pp.231-242.
[27] Ziemian, C.W. and Crawn III, P.M., 2001. Computer aided decision support for fused deposition modeling. Rapid Prototyping Journal, 7(3), pp.138-147.
[28] Rayegani, F. and Onwubolu, G.C., 2014. Fused deposition modelling (FDM) process parameter prediction and optimization using group method for data handling (GMDH) and differential evolution (DE). The International Journal of Advanced Manufacturing Technology, 73(1-4), pp.509-519.
[29] Lee, B.H., Abdullah, J. and Khan, Z.A., 2005. Optimization of rapid prototyping parameters for production of flexible ABS object. Journal of materials processing technology, 169(1), pp.54-61.
[30] Laeng, J., Khan, Z.A. and Khu, S.Y., 2006. Optimizing flexible behavior of bow prototype using Taguchi approach. Journal of Applied Sciences, 6, pp.622-630.
[31] Bertoldi, M., Yardimci, M.A., Pistor, C.M., Guceri, S.I. and Sala, G., 1998. Mechanical characterization of parts processed via fused deposition. Solid Freeform Fabrication Proceedings, Austin, TX, pp.557-565.
[32] Gurrala, P.K. and Regalla, S.P., 2014. Part strength evolution with bonding between filaments in fused deposition modelling: This paper studies how coalescence of filaments contributes to the strength of final FDM part. Virtual and Physical Prototyping, 9(3), pp.141-149.
[33] Croccolo, D., De Agostinis, M. and Olmi, G., 2013. Experimental characterization and analytical modelling of the mechanical behaviour of fused deposition processed parts made of ABS-M30. Computational Materials Science, 79, pp.506-518.
[34] Mahmood, S., Qureshi, A.J., Goh, K.L. and Talamona, D., 2017. Tensile strength of partially filled FFF printed parts: meta modelling. Rapid Prototyping Journal, 23(3), pp.524-533.
[35] Durgun I, Ertan R. Experimental investigation of FDM process for improvement of mechanical properties and production cost. Rapid Prototyping Journal. 2014 Apr 14;20(3):228-35.
[36] Domingo-Espin, M., Puigoriol-Forcada, J.M., Garcia-Granada, A.A., Lluma, J., Borros, S. and Reyes, G., 2015. Mechanical property characterization and simulation of fused deposition modeling Polycarbonate parts. Materials & Design, 83, pp.670-677.
[37] Rezayat, H., Zhou, W., Siriruk, A., Penumadu, D. and Babu, S.S., 2015. Structure–mechanical property relationship in fused deposition modelling. Materials Science and Technology, 31(8), pp.895-903.
[38] Garg, A. and Bhattacharya, A., 2017. An insight to the failure of FDM parts under tensile loading: finite element analysis and experimental study. International Journal of Mechanical Sciences, 120, pp.225-236.
[39] Urbanic, R.J., Hedrick, R.W. and Burford, C.G., 2017. A process planning framework and virtual representation for bead-based additive manufacturing processes. The International Journal of Advanced Manufacturing Technology, 90(1-4), pp.361-376.
[40] Ahn, D., Kweon, J.H., Kwon, S., Song, J. and Lee, S., 2009. Representation of surface roughness in fused deposition modeling. Journal of Materials Processing Technology, 209(15-16), pp.5593-5600.
[41] Bellehumeur, C., Li, L., Sun, Q. and Gu, P., 2004. Modeling of bond formation between polymer filaments in the fused deposition modeling process. Journal of Manufacturing Processes, 6(2), pp.170-178.
[42] Matweb.com. (2018). Online Materials Information Resource - MatWeb. [online] Available at: http://www.matweb.com/ [Accessed 2 Nov. 2018].
[43] ISO, S., 2012. 527-2. Test conditions for moulding and extrusion plastics. Part, 2.
[44] ISO, S., 2012. 527-1. Plastics. Determination of tensile properties. Part, 1.
[45] Wang, E., Nelson, T. and Rauch, R., 2004, May. Back to elements-tetrahedra vs. hexahedra. In Proceedings of the 2004 international ANSYS conference. Pennsylvania: ANSYS.